Supporting Information for "Antarctic Ice Sheet elevation impacts on water isotope records during the Last Interglacial"

Sentia Goursaud[1], Max Holloway[2], Louise Sime[3], Eric Wolff[1], Paul Valdes[4],

Eric J. Steig[5], Andrew Pauling[5]

[1]Department of Earth Sciences, University of Cambridge, UK

[2]Scottish Association for Marine Science, Oban, UK

[3]Ice Dynamics and Paleoclimate, British Antarctic Survey, Cambridge, UK

[4]School of Geographical Science, University of Bristol, Bristol, UK

[5]Department of Atmospheric Sciences, University of Washington, Seattle, US

Contents of this file

Corresponding author: Sentia Goursaud, Department of Earth Sciences, University of Cambridge, UK (sg952@cam.ac.uk)

Introduction This supporting information brings extended analyses to those given in the manuscript.

Text S1: Definition of of water stable isotope. Fractional isotopic content is expressed for oxygen-18 as:

$$\delta^{18}O = 1,000 \times \frac{\frac{H_2^{18}O}{H_2^{16}O}}{R_{VSMOW} - 1} \tag{1}$$

in ‰, where R_{VSMOW} is the ratio of $H_2^{18}O$ to $H_2^{16}O$

Text S2: Extended description of elevation relationships.

We first calculated linear least squares regression between a climate variable Y - the surface air temperature (SAT), precipitation, or $\delta^{18}O$ - and the elevation X for each grid of the model. Each pair of points (x_i, y_i) corresponds to anomalies of an idealised simulation against a Pre-Industrial (PI) control simulation (see Table S1). The problem is to minimise the residual E of the sum of the squares of the differences between the points of the climate variable (the SAT or the precipitation or the $\delta^{18}O$) and the elevation points, such as:

$$E = \sum_{i=0}^{n} (y_i - (ax_i + b))^2 \tag{2}$$

with y_i the points of the considered climatic variable and x_i the elevation points.

The solutions of the slope a and the intercept b are given by:

$$a = \frac{\sum_{i=0}^{n}(x_i - \bar{x})(y_i - \bar{y})}{\sum_{i=0}^{n}(x_i - \bar{x})^2} \tag{3}$$

$$b = \bar{y} - a\bar{x} \tag{4}$$

and the quality of the regression is given by the correlation coefficient r_{xy}, such as:

$$r_{xy} = \frac{cov_{xy}}{sxsy} \tag{5}$$

with

$$cov_{xy} = \frac{1}{n}\sum_{i=0}^{n}(x_i - \bar{x})(y_i - \bar{y}) \tag{6}$$

$$s_x^2 = \frac{1}{n}\sum_{i=0}^{n}(x_i - \bar{x}) \tag{7}$$

The regression is considered significant when the p-value is below 0.05.

We then averaged the slopes and the correlation coefficents for different elevation ranges (see Table S3), by weighting by the grid area. Non significant relationships were excluded from the averages.

Text S3: Comparison of the Talos Dome ice core record imprint on the local LIG elevation. Sutter et al. (2020) compared the elevation-inferred δ^{18}O from the Parallel Ice Sheet Model (PISM) simulations, applying a subshelf melting perturbation to the ice shelves of the George V and Sabrina Coast during the Last Interglacial. Looking at different grid resolution (4-,8-, and 16-km), they observe two stable modes: (i) a stabilized grounding line due to the rebounding bedrock as well as the reformation of ice shelves, and (ii) a runaway retreat leading to a substantial reduction by more than 1000 m elevation at Talos Dome. In the second case, using the present-day SAT versus elevation relationship of 0.8 K/100 m (Frezzotti et al., 2007) multiplied by the SAT versus temperature relationship of 0.66 ° C/‰ derived from Werner, Jouzel, Masson-Delmotte, and Lohmann (2018) for Talos Dome at the Last Glacial Maximum (using Last Glacial Maximum (LGM) simulations processed by the ECHAM5-wiso model), they could infer expected δ^{18}O changes ranging between 6 and 11 ‰.

Using the same relationships, we deduced their extrema simulated elevations. We found elevation changes ranging from 1136 to 2075 m. Then, using our Last Interglacial δ^{18}O versus elevation relationships of -0.93 ‰/100 m for Talos Dome (see Table 7), we infer corrected δ^{18}O

changes for the Last Interglacial. We found δ^{18}O changes ranging between 11 and 19 ‰. If we assume our simulations not to be biased due to a coarse resolution grid, this result would show a net underestimation of the inferred δ^{18}O from the grounding retreat mode (ii) found in Sutter et al. (2020), even more unequivocally excluding it when comparing it with the δ^{18}O changes (compared to PI) from the observational records of 2 ‰ (Masson-Delmotte et al., 2008).

References

Bazin, L., Landais, A., Lemieux-Dudon, B., Toyé Mahamadou Kele, H., Veres, D., Parrenin, F., ... Wolff, E. (2013). An optimized multi-proxy, multi-site antarctic ice and gas orbital chronology (aicc2012): 120ndash;800 ka. *Climate of the Past*, *9*(4), 1715–1731. Retrieved from https://cp.copernicus.org/articles/9/1715/2013/ doi: 10.5194/cp-9-1715-2013

Frezzotti, M., Urbini, S., Proposito, M., Scarchilli, C., & Gandolfi, S. (2007). Spatial and temporal variability of surface mass balance near talos dome, east antarctica. *Journal of Geophysical Research: Earth Surface*, *112*(F2).

Masson-Delmotte, V., Buiron, D., Ekaykin, a., Frezzotti, M., Gallée, H., Jouzel, J., ... Vimeux, F. (2011, apr). A comparison of the present and last interglacial periods in six Antarctic ice cores. *Climate of the Past*, *7*(2), 397–423. Retrieved from http://www.clim-past.net/7/397/2011/ doi: 10.5194/cp-7-397-2011

Masson-Delmotte, V., Hou, S., Ekaykin, A., Jouzel, J., Aristarain, A., Bernardo, R. T., ... White, J. W. C. (2008, jul). A Review of Antarctic Surface Snow Isotopic Composition: Observations, Atmospheric Circulation, and Isotopic Modeling. *Journal of Climate*, *21*, 3359–3387. Retrieved from http://journals.ametsoc.org/doi/abs/10.1175/2007JCLI2139.1 doi: 10.1175/2007JCLI2139.1

Sutter, J., Eisen, O., Werner, M., Grosfeld, K., Kleiner, T., & Fischer, H. (2020). Limited retreat of the wilkes basin ice sheet during the last interglacial. *Geophysical Research Letters*, *47*(13), e2020GL088131.

Werner, M., Jouzel, J., Masson-Delmotte, V., & Lohmann, G. (2018). Reconciling glacial

antarctic water stable isotopes with ice sheet topography and the isotopic paleothermometer. *Nature Communications*, *9*(3537).

Table S1. Model Simulations. Experiment name ("Experiment"), run duration ("Duration" in years), year for the orbital configuation ("Orbit" in kyears BP), and elevation change compared to EDC ("EDC Δz" in meter). All simulations were carried out using HadCM3.

Experiment	Duration (yrs)	Orbit (ka)	EDC Δz (m)
PI	700	0	0
LIG	700	128	0
Flat WAIS	700	128	0
DC+1km	500	128	+1000
DC+500m	500	128	+500
DC+200m	500	128	+200
DC+100m	500	128	+100
DC-100m	500	128	-100
DC-200m	500	128	-200
DC-500m	500	128	-500
DC-1km	500	128	-1000

Table S2. Time averaged values over the whole Antarctic. Surface air temperature ("SAT" in ° C), precipitation ("P" in mm/month) and δ^{18}O in the precipitations (in ‰) area-weighted averaged over the last 50 simulated years and the whole Antarctic, associated with the standard value of all the grid points (average ± standard deviation).

Experiment	SAT (° C)	P (mm/month)	δ^{18}O (‰)
PI	-36.8 ± 11.8	14.5 ± 15.9	-40.3 ± 12.3
LIG	-35.9 ± 11.8	15.1 ± 16.1	-39.7 ± 12.7
DC+1km	-40.3 ± 15.7	12.7 ± 16.8	-42.6 ± 13.3
DC+500m	-38.2 ± 13.8	13.9 ± 16.5	-41.6 ± 13.3
DC+200m	-36.7 ± 12.6	14.7 ± 16.3	-40.4 ± 12.9
DC+100m	-36.4 ± 12.3	14.9 ± 16.3	-40.0 ± 12.8
DC-100m	-35.5 ± 11.4	15.4 ± 16.1	-39.1 ± 12.4
DC-200m	-34.9 ± 10.9	15.9 ± 15.9	-38.6 ± 12.2
DC-500m	-33.5 ± 9.7	16.7 ± 15.8	-36.8 ± 11.5
DC-1km	-31.4 ± 7.7	18.1 ± 15.3	-33.8 ± 10.0

Table S3. δ^{18}O ice core anomalies against PI. Observed and modeled δ^{18}O ice core values for the PI and the LIG, as well as δ^{18}O ice core anomalies of our idealised simulations as described in Table S1 as well and the 200 m WAIS simulation ("Flat WAIS") analysed in Holloway et al. (2016), against the PI control simulation for the ice core locations of Vostok, Dome F, EPICA Dome C (EDC), EPICA Dronning Maud Land (EDML), Talos Dome (TALDICE) and Taylor Dome, in ‰. The observed values were extracted from Bazin et al. (2013), thus aligned on the AICC2012 when available (for EDML and Taldice) and Masson-Delmotte et al. (2011) otherwise, thus aligned on the EDC3 chronology. The observed PI value corresponds to the average over the period 1850-1900, and the LIG value corresponds to the maximum value during the LIG period.

Ice core site	Vostok	Dome F	EDC	EDML	TALDICE	Taylor Dome	WAIS Divide	Hercules Dome	Skytrain
Observed PI	-57.1	-55.2	-50.3	-45.4	-36.2	-40.0			
Observed LIG	-53.8	-50.7	-46.3	-42.5	-33	-38.1			
Modeled PI	-55.3	-54.8	-51.1	-44.9	-37.7	-42.8	-34.6	-47.3	-29.8
Modeled LIG	-56.8	-54.9	-51.8	-44.5	-37.4	-43.4	-33.5	-46.7	-29.3
DC+1km	-2.1	-0.8	-3.2	-1.1	-3.9	-2.8	-3.3	-4.2	-2.5
DC+500m	-3.6	-2.2	-3.7	-0.5	-2.9	-2.3	-1.0	-1.9	-0.7
DC+200m	-2.1	-0.8	-1.6	0.6	-1.1	-1.6	0.1	-0.2	-0.1
DC+100m	-1.5	-0.3	-1.2	0.0	0.4	-0.2	0.8	0.4	0.8
DC-100m	0.1	0.9	1.3	1.4	1.4	0.5	1.7	1.6	1.8
DC-200m	0.7	1.5	2.0	1.7	2.0	0.3	1.9	2.2	1.7
DC-500m	3.0	4.5	4.7	3.5	3.8	2.5	3.1	4.1	2.8
DC-1km	8.0	9.5	9.7	8.1	7.5	5.6	5.2	7.5	4.5
Flat WAIS	-0.2	0.5	0.0	1.1	0.2	-0.4	13.4	14.5	11.4

Table S4. Changes in the regional sea ice extents. Sea ice extent changes (%) when compared to the LIG experiment. The sectors are defined as follows: the Eastern sector (0–180° E), the Weddell sector (60–30° W), the Bellingshausen sector (100–75° W), the Ross sector (180–145° W) and the Pacific sector (180–75° W)

Sector	DC-1km	DC-500m	DC-200m	DC-100m	DC+100m	DC+200m	DC+500m	DC+1km
Bellingshausen	50.0	0.0	0.0	14.3	0.0	0.0	-7.1	0.0
Ross	1.6	1.6	0.0	0.0	-1.6	-1.6	-1.6	-12.5
Pacific	12.8	2.6	0.9	4.3	-1.7	-4.3	-7.7	-16.2
Weddel	-1.2	-3.7	-2.4	3.7	0.0	-2.4	-4.9	-4.9
East	6.9	2.5	0.0	0.0	-1.9	-1.9	-6.9	-10.1
All	7.6	1.1	-0.2	2.3	-1.4	-2.5	-6.0	-10.8

Table S5. Elevation relationships. Area weighted averages and standard deviations of the slopes ("Slope", in units /100 m) and correlation coefficients ("r") between the deviations (each DC experiment compared to the LIG simulation) of surface air temperature ("SAT" in °), precipitation ("P" in mm/month) and δ^{18}O (in ‰) and the evelation for each grid point. Averages are calculated for different elevation ranges: above 3000 m a.s.l ("≥3000m"), between 2000 and 3000 m a.s.l ("2000-3000m"), between 1000 and 2000 m a.s.l ("1000-2000m") and below 1000 m a.s.l ("≤1000m"). This table Supplements Figure 3 in the manuscript.

	SAT		P		δ^{18}O	
	Slope	r	Slope	r	Slope	r
≥3000m	-0.92 ± 0.11	-1.0 ± 0.0	-0.22 ± 0.09	-0.96 ± 0.02	-0.53 ± 0.22	-0.84 ± 0.3
2000-3000m	-0.75 ± 0.19	-1.0 ± 0.01	-0.46 ± 0.32	-0.92 ± 0.25	-0.71 ± 0.15	-0.96 ± 0.06
1000-2000m	-0.34 ± 0.24	-0.80 ± 0.44	-1.12 ± 1.24	-0.64 ± 0.61	-0.93 ± 0.28	-0.98 ± 0.06
100-1000m	0.31 ± -1.47	0.16 ± 0.8	0.21 ± 5.41	-0.14 ± 0.88	-1.28 ± 1.38	-0.78 ± 0.52
≤1000m	-8.99 ± 341.02	0.16 ± 0.78	17.47 ± 283.15	-0.09 ± 0.85	-13.28 ± 201.28	-0.62 ± 0.64
≤100m	-71.2 ± 943.23	0.19 ± 0.71	132.93 ± 775.2	-0.08 ± 0.64	-92.93 ± 549.69	0.03 ± 0.63

Table S6. Ice core elevation relationships. Simulated slopes ("Slope") and square of the correlation coefficient of surface air temperaturs versus elevation relationships ("SAT", in °C/100 m), as well as of δ^{18}O versus elevation relationships (δ^{18}O/100 m) for the grid points corresponding to Vostok, Dome F, EDC, EDML, TALDICE, Taylor Dome, WAIS, Hercules Dome and Skytrain. The SAT-elevation relationship for Skytrain is not given as it is not significant.

	SAT		δ^{18}O	
	Slope	r^2	Slope	r^2
Vostok	-0.91	0.99	-0.49	0.79
Dome F	-0.97	0.99	-0.51	0.77
EDC	-1.1	1.00	-0.69	0.88
EDML	-0.9	1.00	-0.48	0.84
TALDICE	-0.55	0.99	-0.93	0.97
Taylor Dome	-0.29	0.99	-0.79	0.92
WAIS Divide	-0.32	0.93	-0.76	1.00
Hercules Dome	-0.53	0.99	-0.79	0.99
Skytrain			-3.52	0.99

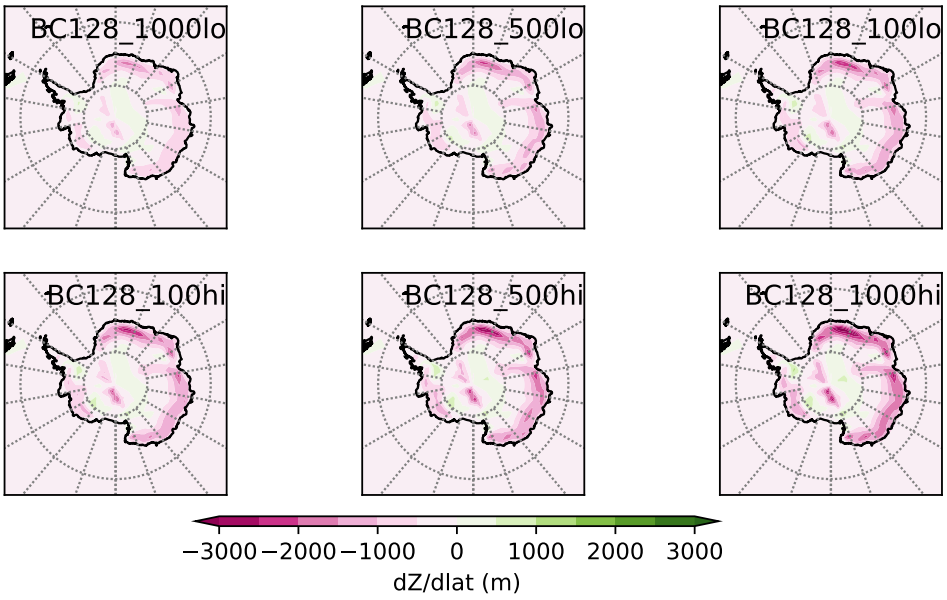

Figure S1. Steepness of the Antarctic topography. Steepness of the Antarctic topography as calculated by the difference between the elevation of each considered grid and the one of higher latitude and same longitude.

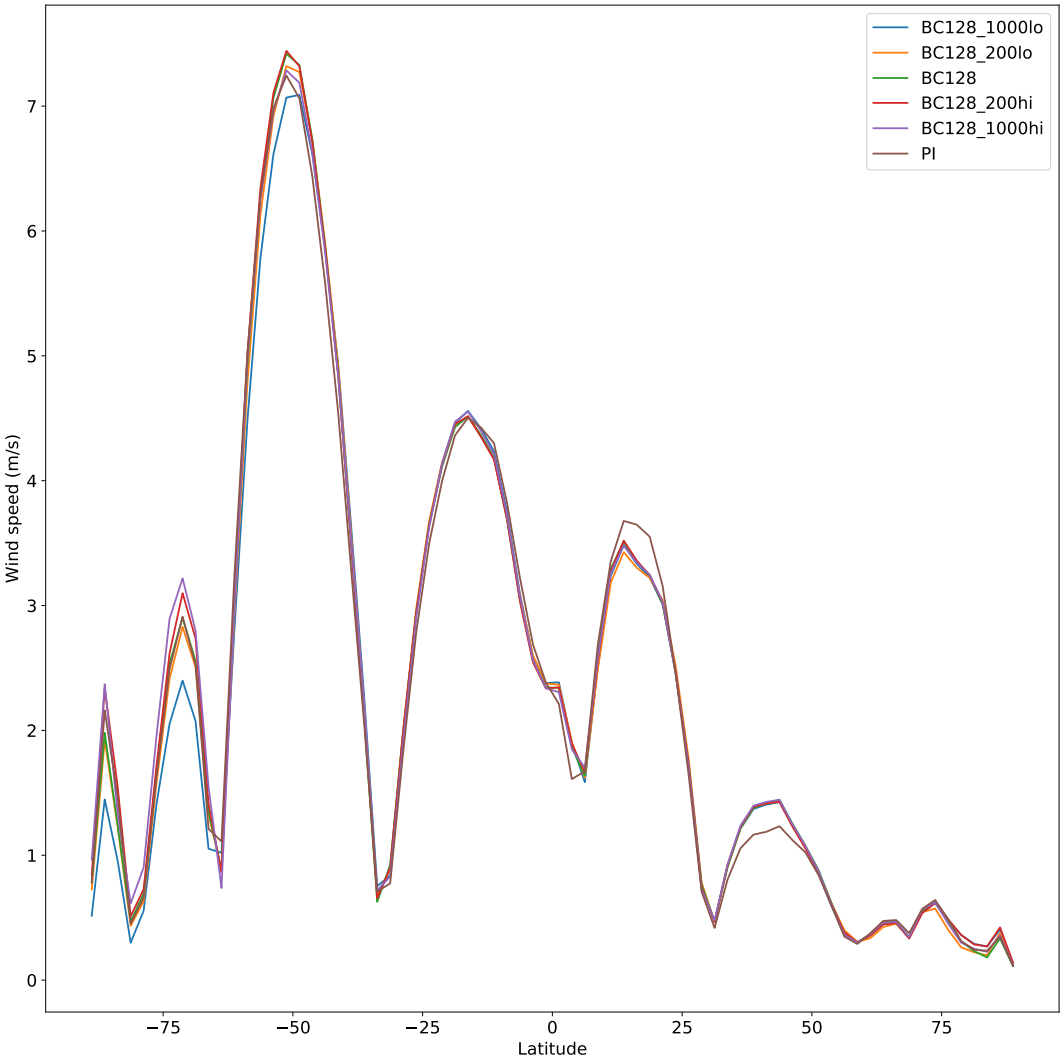

Figure S2. Surface wind speeds. Surface wind speed (in m/s) vs latitudes for the Preindustrial ("PI", in brown), Last Interglacial ("BC128", in green), DC-1000 ("BC128_1000lo", in blue), DC-200 ("BC128_200lo", in orange), DC+200 ("BC128_200hi", in red), and DC+1000 ("BC128_1000hi", in purple) simulations.

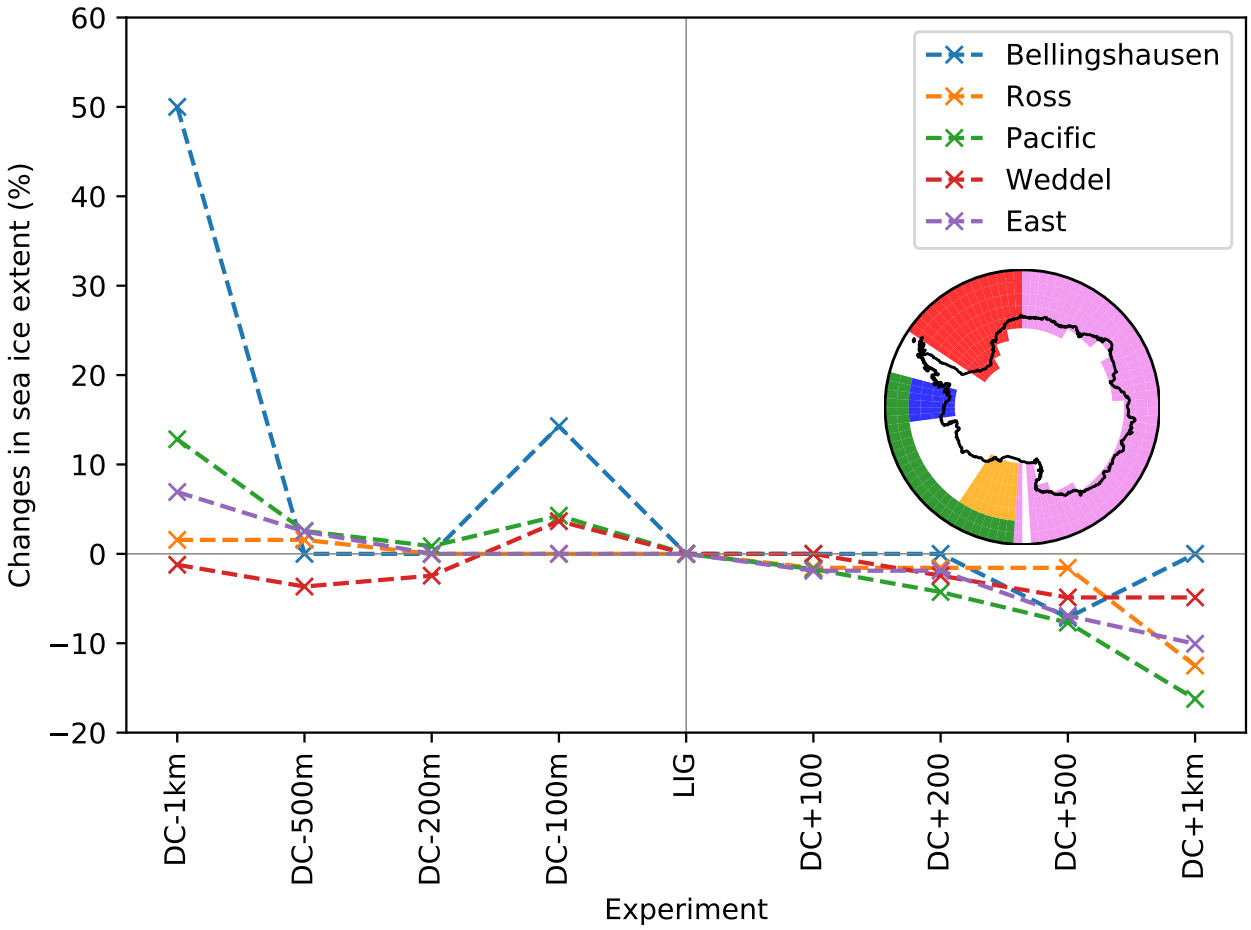

Figure S3. Changes in the regional sea ice extents. Changes in sea ice extent (in %) vs changes in elevation (in m) when compared to the BP128 experiment. The sectors are defined as follows: the Eastern sector (0–180° E), the Weddell sector (60–30° W), the Bellingshausen sector (100–75° W), the Ross sector (180–145° W) and the Pacific sector (180–75° W).

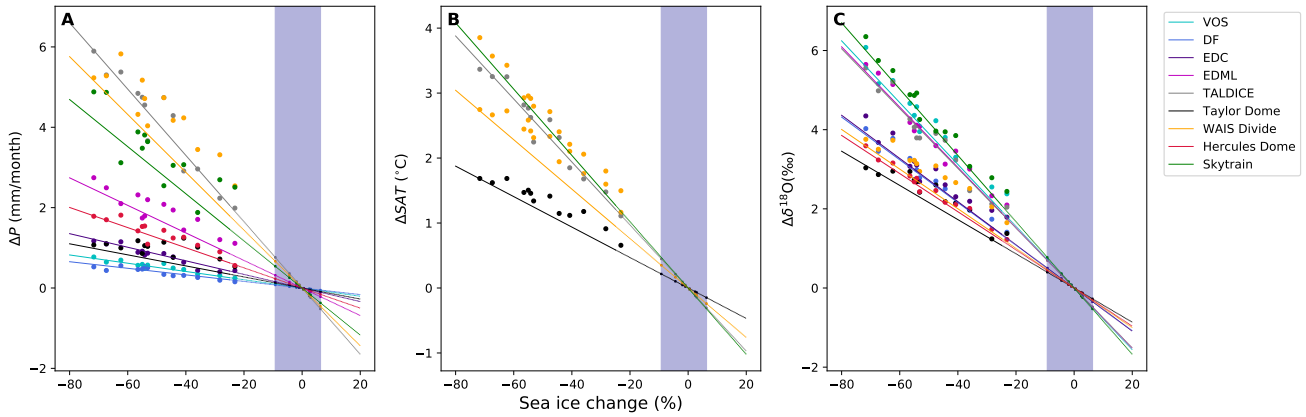

Figure S4. Sea ice corrections. Deviations of simulated precipitations ("P" in mm/month, panel A), surface air temperature ("SAT" in °C, panel B), and δ^{18}O in the precipitations (in ‰, panel C) compared to the Last Interglacial control simulation, against changes in sea ice extent (in %) compared to the Last Interglacial control simulation, using the sea ice reduction sensitivity simulations from Holloway et al. (2016) for each ice core location. Dots display outputs from the sea ice reduction sensitivity tests; the lines show the significant linear regressions against the sea ice changes; the blue shadow indicate the range of our Antarctic Ice Sheet simulations; and little squares the outputs from our Antarctic Ice Sheet simulations.